L.N.L. - I.N.F.N. (REP) 73 / 93

Studies of Subbarrier Fusion in Heavy Ion Reaction leading to 118,122,128 *Ba* as Compound Nuclei#

D. Ackermann, P. Bednarczyk, L. Corradi, D.R. Napoli, C.M. Petrache, P. Spolaore, A.M. Stefanini, H.Zhang, F. Scarlassara, S. Beghini, G. Montagnoli, L. Müller, G.F. Segato, C. Signorini.

Istituto Nazionale di Fisica Nucleare, Laboratori Nazionali di Legnaro i- 35020 Legnaro Padova Italy

Dipartimento di Fisica , Università di Padova, and I. N.F.N. , Sezione di Padova

To be bublished in the proceedings to the " Second Europea Bienniel Workshop on Nuclear Physics" - Mégeve, 29 March - 2 May 1993

A cura del servizio
Documentazione dei
L.N.L.

L.N.L. - I.N.F.N. (REP) 73 / 93

Studies of Subbarrier Fusion in Heavy Ion Reactions leading to $^{118,122,128}Ba$ as Compound Nuclei#

D. Ackermann*, P. Bednarczyk†, L. Corradi, D.R. Napoli,
C.M. Petrache‡, P. Spolaore, A.M. Stefanini, H. Zhang§
Istituto Nazionale di Fisica Nucleare, Laboratori Nazionali di Legnaro, I-35020 Legnaro Padova, Italy
F. Scarlassara, S. Beghini, G. Montagnoli,
L. Müller, G.F. Segato, C. Signorini
Dipartimento di Fisica, Università di Padova, and Istituto Nazionale di Fisica Nucleare, Sezione di Padova, I-35100 Padova, Italy

To be published in the proceedings to the "Second European Bienniel Workshop on Nuclear Physics" - Megéve, 29. March – 2. May 1993

A cura del servizio
Documentazione dei
L.N.L.

Studies of Subbarrier Fusion in Heavy Ion Reactions leading to $^{118,122,128}Ba$ as Compound Nuclei#

D. Ackermann,* P. Bednarczyk,† L. Corradi, D.R. Napoli,
C.M. Petrache,‡ P. Spolaore, A.M. Stefanini, H. Zhang§
Istituto Nazionale di Fisica Nucleare, Laboratori Nazionali di Legnaro, I-35020 Legnaro Padova, Italy
F. Scarlassara, S. Beghini, G. Montagnoli,
L. Müller, G.F. Segato, C. Signorini
Dipartimento di Fisica, Università di Padova, and Istituto Nazionale di Fisica Nucleare, Sezione di Padova, I-35100 Padova, Italy

Abstract

Fusion cross sections and mean angular momenta have been measured for the reactions $^{58}Ni+^{60}Ni$ and $^{58,64}Ni+^{64}Ni$ at energies ranging from $\approx 10\% - 15\%$ above to $\approx 10\%$ below the Coulomb barrier. Barrier distributions have been extracted directly from the fusion excitation functions. The influence on fusion of transfer channels with $Q = 0$, $Q < 0$ and $Q > 0$ shows up clearly with different signatures in the barrier distributions.

Contents

*Supported by a grant of the Commission of the European Communities
†on leave from *Inst. of Nucl. Phys., Cracow, Poland*
‡on leave from *Inst. of Phys. and Nucl. Eng., Bucarest, Romania*
§on leave from *Inst. for Atomic Energy, Beijing, China*

1 Introduction

Early experiments dealing with subbarrier heavy ion fusion, more than ten years ago, had shown that the picture of tunneling through a one-dimensional barrier was not sufficient to explain the obtained cross sections at low energies. Soon it became clear that the mechanism of nuclear interaction is complex and the picture had to be extended to a more complicated potential landscape, consisting of a superposition of many barriers. In case of deformed nuclei both barrier height and radius depend on the orientation of the symmetry axis relative to the beam direction. Integrating over all these possible barriers the enhancement of the fusion

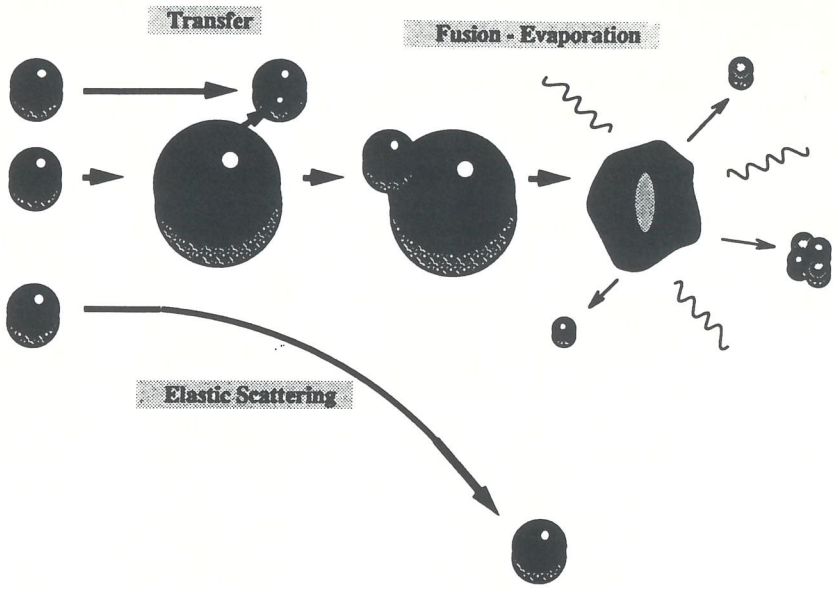

Figure 1: *HI collision close to the Coulomb barrier. The various reaction channels fusion, transfer and nuclear excitation interact with each other.*

cross sections for the deformed ^{154}Sm in collisions with different spherical partners could be reproduced [1, 2, 3]. But also the influence of other reaction channels, as e.g. inelastic excitation of low-energy collective vibrations and nucleon transfer, has been established in various cases. Fig. 1 is a pictoral view of the situation in the vicinity of the Coulomb barrier. The interplay between the entrance channel and the various reaction channels changes the inter-nuclear potential landscape. In this way quasi-elastic transfer and/or nuclear excitations can act as doorway-states driving fusion. In various cases coupled channels calculations give fusion cross sections fairly close to the experimental values, as e.g. for $^{28,30}Si + ^{58,62,64}Ni$ and $^{32,34,36}S + ^{58,64}Ni$ investigated by A.M. Stefanini et al. [5]. Those data could be reproduced reasonably taking into account the coupling to the lowest excited states of the colliding nuclei and the transfer of two neutrons as can be seen in fig. 2 for the cases $S + Ni$.

Another interesting evidence of coupled channels effects in low-energy heavy-ion reactions comes from the observation of the socalled threshold anomaly of

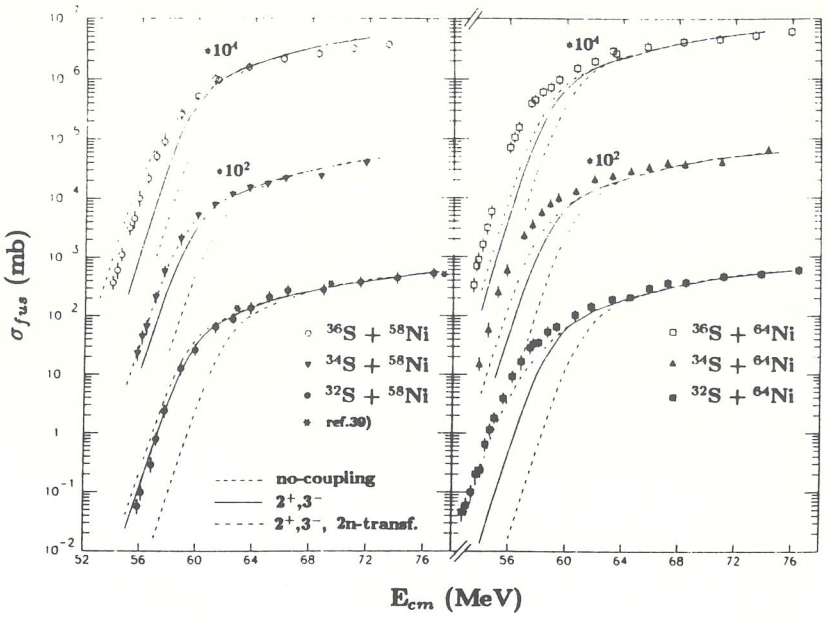

Figure 2: *Fusion cross sections for* $^{32,34,36}S + ^{58,64}Ni$.

the optical potential describing elastic scattering near the barrier. The classical example is $^{16}O + ^{208}Pb$, where elastic cross sections could be explained considering both nuclear excitations and nucleon transfer. The coupled states are shown in fig. 3 [4].

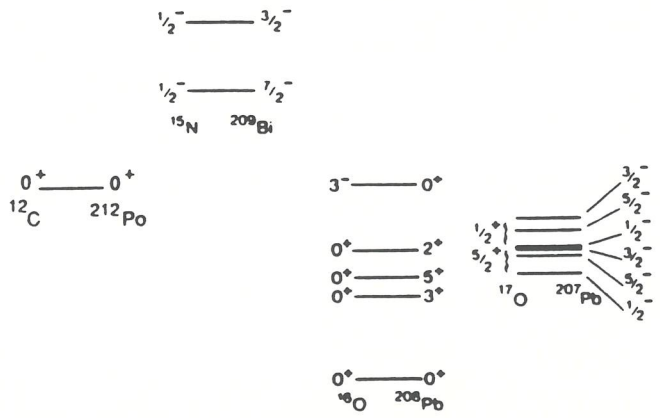

Figure 3: *The coupled channels used in the analysis for the reaction* $^{16}O + ^{208}Pb$ *from reference [4].*

In recent years another parameter which is strongly connected with the fusion cross section has become accessible. Average angular momenta $< l >$ and even complete spin distributions $\sigma_l(E)$ have been measured by means of γ-detector arrays. DiGregorio et al. gave in reference [7] an overview over the present situation comparing theoretical and experimental values for both fusion cross sections σ_{fus} and $< l >$. This comparison calls for a dependence on the mass asymmetry in the entrance channel: i.e. asymmetric systems are well explained whereas for symmet-

ric ones coupled channel calculations have severe problems in the region below the Coulomb barrier.

Apart from this a lack of precise information about the identification and coupling strengths of the channels driving fusion is strongly felt.

A recent developement however, allows a direct insight in the potential landscape created by the specific reaction interplay: N. Rowley et al. [8] (see chapter 3) proposed the extraction of the distribution of the barriers deriving two times the excitation function. In this way a clear identification of the channels which act as main doorway states for fusion has become possible in various cases [9].

We measured σ_{fus} and $<l>$ for $^{58,64}Ni+^{64}Ni$ and σ_{fus} for $^{58}Ni+^{60}Ni$ with high accuracy. These systems display some interesting and different features concerning the sign of the ground state Q-value of neutron transfer channels.

- For $^{58}Ni+^{64}Ni$ Broglia et al. [10] pointed to the dominant influence of the available $2n$-transfer channel with positive Q on the observed fusion enhancement.
- In the case of $^{64}Ni+^{64}Ni$ all transfer channels have negative Q-value.
- $^{58}Ni+^{60}Ni$ has obviously a 2n-transfer channel with $Q = 0$.

2 Experimental set-up

The main part of the experiment has been carried out at the L.N.L. recoil mass spectrometer (RMS) (fig. 4). For the system $^{58}Ni+^{60}Ni$ we have used the eletrostatic deflector set-up [11] in an improved version. The beams of $^{58,64}Ni$ ions with energies ranging from $174MeV$ to $222MeV$, in pulses $3ns$ to $10ns$ wide and $800ns$ apart (in case of the RMS set-up only), were delivered by the XTU tandem accelerator. We irradiated ^{64}Ni and ^{60}Ni targets with a thicknesses of $320\mu g/cm^2$ and $100\mu g/cm^2$, respectively. Two silicon surface barrier detectors were placed at $\pm 30°$ with respect to the beam direction for normalization and beam control purposes. A detailed description of the spectrometer is given in ref. [12]. The RMS provides $\frac{M}{q}$ dispersion at the focal plane with a mass resolution of $> \frac{1}{300}$ and performs a first separation of ER from scattered beam particles. The final separation is done by measuring the time of flight (ToF) of the particles through the spectrometer and their kinetic energy. The ER were detected at the focal plane by a multiwire parallel plate avalanche counter (MW-PPAC) incorporated in a Bragg chamber. This detector yields x- and y-position, ΔE and E of the ions. More detailed information can be found in ref. [13]. The total set-up efficiency was measured comparing characteristic γ-transitions of the ER, counted in a Ge-detector placed at 90° close to the target, with and without coincidence with the ER detected at the focal plane.

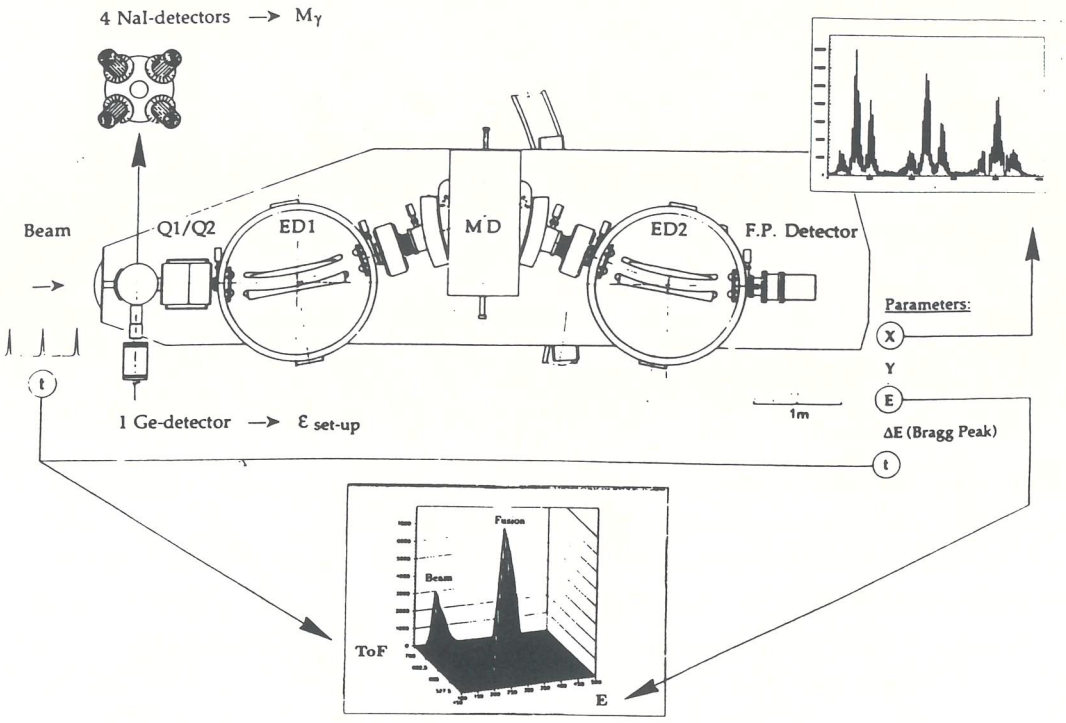

Figure 4: *The recoil mass spectrometer (RMS) with the detector system (see text and ref. [12]).*

In fig. 5a) a three-dimensional plot of the ToF-energy plane is shown for $^{58}Ni+^{64}Ni$ at a beam energy of $212.3MeV$. The reaction products are well separated by a quite wide valley from the scattered beam particles. In part b) of this figure the mass spectrum for this case is shown with a gate on the reaction products in the ToF-plane as condition. The three charge states 25^+, 26^+ and 27^+ (from the right to the left) fit in the focal plane of $120mm$ width. The three masses populated in this reaction are clearly resolved in all three charge states. The main reaction channel ^{119}Xe, which is the residue from a $2pn$-evaporation of the compound nucleus ^{122}Ba, is contained in the central peak (mass 119). The left peak corresponds to mass 120, and the right one to mass 118.

3 Barrier distributions $D(B)$

N. Rowley et al. [8] proposed recently a method to extract barrier distributions directly from the fusion excitation function. Assuming the cross section $\sigma(E)$ as the integral over the local cross sections $\sigma(E,B)$ multiplied with the weight function $D(B)$ over all barriers

$$\sigma(E) = \int_0^\infty \sigma(E,B)D(B)dB, \qquad (1)$$

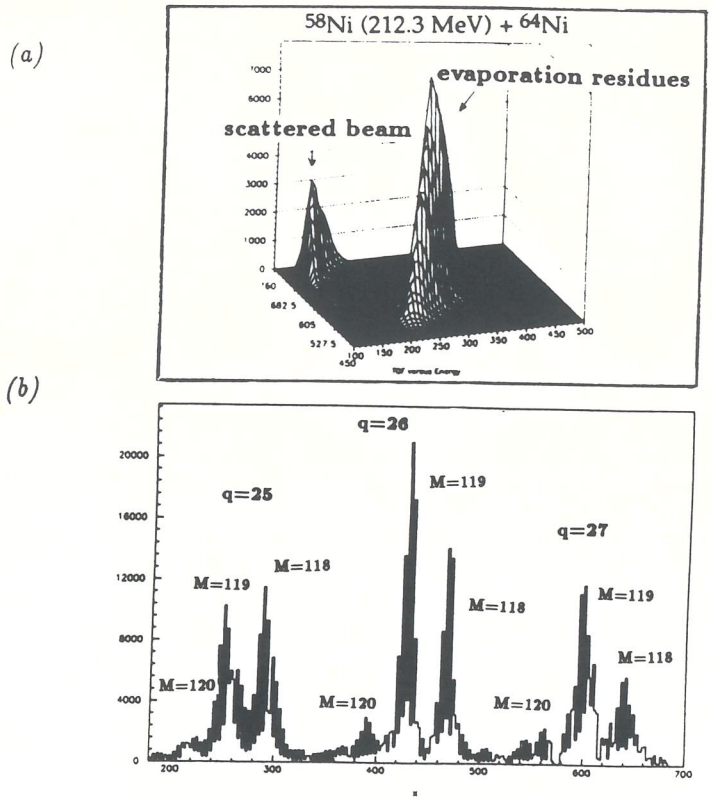

Figure 5: *ToF-energy plot (a) and mass spectrum (b) for the reaction* $^{58}Ni(212.3MeV) + ^{64}Ni$.

where E is the kinetic energy and B the single barrier, and using the classical fusion cross section

$$\begin{aligned} E\sigma(E,B) &= \pi R^2(E-B) \quad |\text{for } E > B \text{ and} \\ E\sigma(E,B) &= 0 \qquad\qquad |\text{for } E < B, \end{aligned} \tag{2}$$

they apply the first and second derivative on the function $E\sigma(E,B)$. The first derivative gives some information about the localisation of the mean barrier $\bar{B}$ and the interaction radius R

$$\begin{aligned} \frac{dE\sigma(E,B)}{dE} &= \pi R^2 \quad |\text{for } E > B \text{ and} \\ \frac{dE\sigma(E,B)}{dE} &= 0 \qquad |\text{for } E < B. \end{aligned} \tag{3}$$

The second derivative of this step function gives the Dirac-δ function

$$\frac{d^2E\sigma(E,B)}{dE^2} = \pi R^2\delta. \tag{4}$$

If we now introduce the quantum tunneling through the barrier and assume for the cross section the Wong formula [14]

$$\sigma_w = \frac{\hbar\omega}{2E}R^2[1+\exp(\frac{2\pi}{\hbar\omega}(E-B))], \tag{5}$$

the δ becomes a Gaussian. The coupling to various channels and the consequent presence of a number n of barriers result in the superposition of n Gaussians weighted according to their strength

$$\frac{d^2E\sigma(E,B)}{dE^2} = \pi R^2 \sum_{i=1}^{n} w_i G(x_i), \tag{6}$$

which represents the barrier distribution

$$\frac{d^2E\sigma(E,B)}{dE^2} = \pi R^2 D(B). \tag{7}$$

3.1 Coupled channels prediction

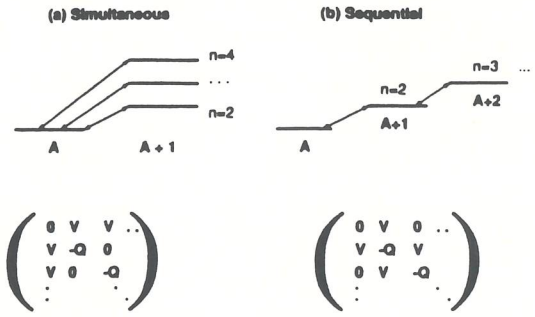

Figure 6: *Two possible types of transfer coupling [15].*

Exact coupled channel calculations [16] were also performed and barrier distributions were derived for various cases [15]. In fig. 7 the results for $^{16}O + ^{17}O$ are shown for the coupling to nucleon transfer channels with positive, negative Q-values and $Q = 0$. Two cases are considered: simultaneous and sequential coupling, schematically shown in fig. 6 with the corresponding coupling matrices. The barrier distributions depend significantly on the Q-value, i.e. the centroid of the distributions are at energies lower than the nominal barrier for $Q < 0$, and viceversa for $Q > 0$, both in the case of simultaneous and in that of sequential coupling. The shape for the simultaneous zero-energy coupling shows a pronounced double humped structure, whereas the presence of $Q = 0$ sequential coupling results in a wide and flat distribution.

3.2 Interaction radii (πR^2) and mean barriers $\bar{B}$

As mentioned above the first derivative of the function $E \times \sigma$ provides useful information about barrier position and interaction cross section πR^2. The latter can be derived also applying directly equation 2. This is done for the three systems we measured in fig. 8a). The function is well defined only for $E > B$ and saturates

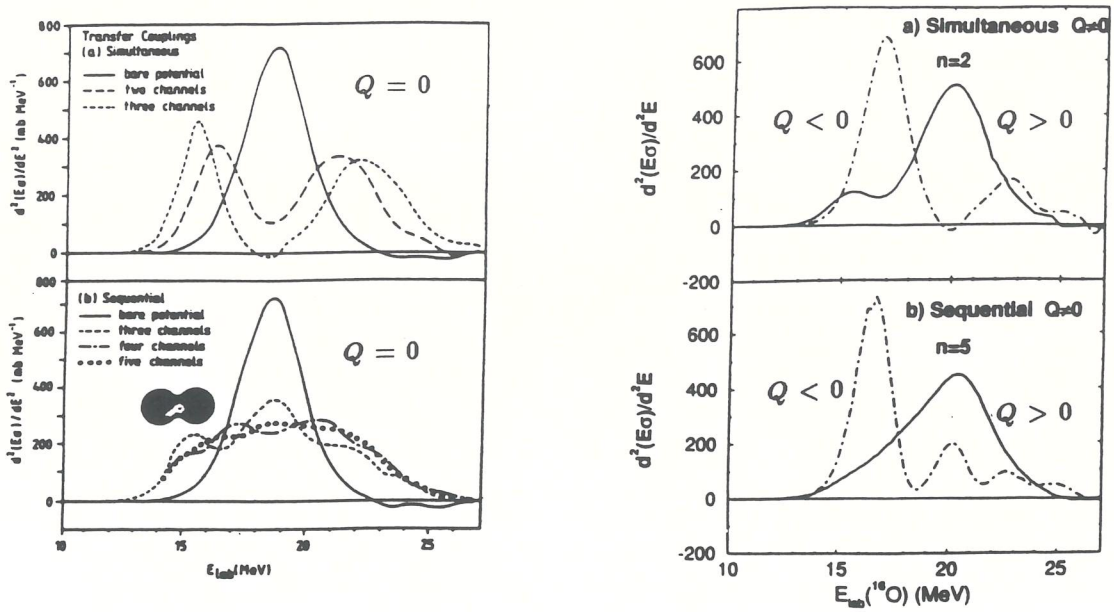

Figure 7: *Barrier distributions obtained from coupled channel calculations for the coupling to transfer channels under various conditions [15]:*
a) *Simultaneous transfer.*
b) *Sequential transfer.*

for all three systems above a value of $3000mb$ that corresponds to an interaction radius of $\approx 10fm$. In part b) of this figure the first derivatives of $E \times \sigma$ normalized to πR^2 are shown. The mean barriers for the three systems are indicated by arrows.

3.3 D(B) for $^{58}Ni+^{60}Ni$ and $^{58,64}Ni+^{64}Ni$

We extracted the barrier distributions shown in fig.9 from the fusion excitation function taking into account only the statistical errors and those for the background subtraction. A systematical error of 15%, which is due to the uncertainty in the efficiency measurement, is supposed to be constant and has therefore no effect on the shape of the excitation function. The barrier distributions have been obtained from the data as the second derivative of the function $E\sigma(E,B)$. So they show, especially in the high energy part, large errors, but this has no influence on the interpretation in the barrier region.

The three systems show significantly different behaviours and allow a clear interpretation concerning the specific channels driving fusion:

- The distribution for the system $^{64}Ni+^{64}Ni$ is peaked at energies lower than the marked mean barrier. According to what we discussed above, this leads to the conclusion that here channels with negative Q-value are mainly important for the low energy fusion process. Following the argumentation in

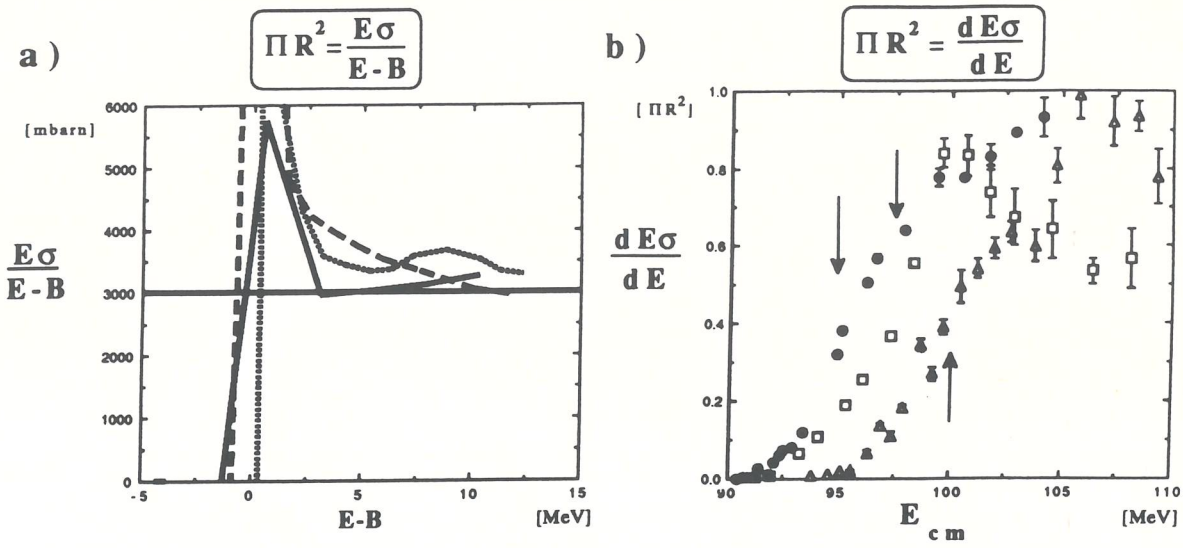

Figure 8: *Barrier localisation and interaction cross section:*
a) πR^2 *derived directly from the classical fusion cross section. The horizontal line indicates a cross section of 3000mb that corresponds to an interaction radius of* $\approx 10fm$. $^{64}Ni+^{64}Ni$ *solid line ,* $^{58}Ni+^{64}Ni$ *broken line and* $^{58}Ni+^{64}Ni$ *dotted line.*
b) *First derivative of* $E \times \sigma$ *normalized to* πR^2. *The arrows indicate the mean barriers* $\bar{B}$ *for the three systems from the left to the right:* $^{64}Ni+^{64}Ni$ *(dots),* $^{58}Ni+^{64}Ni$ *(squares) and* $^{58}Ni+^{60}Ni$*(triangles).*

reference [15], this would indicate the formation of a neck between the two colliding nuclei as driving force for fusion.

- In the case of $^{58}Ni+^{64}Ni$ on the contrary, the barrier distribution is clearly peaked on the high energy side and calls therefore for a strong coupling to the 2n-transfer channel with positive Q.
- For $^{58}Ni+^{60}Ni$ the shape is clearly double humped and thus indicates that in this case an adiabatic channel with simultaneous coupling is most important. The 2n-transfer reaction $^{60}Ni(^{58}Ni,^{60}Ni)^{58}Ni$ has of course $Q = 0$. Therefore we have a strong indication that the elastic transfer is strongly coupled and determines the low-energy fusion process.

4 Conclusions and first applications

The method of extracting barrier distributions from measured fusion excitation functions discussed here is a useful tool to investigate the complex interaction between the various reaction channels in the energy range close to the Coulomb

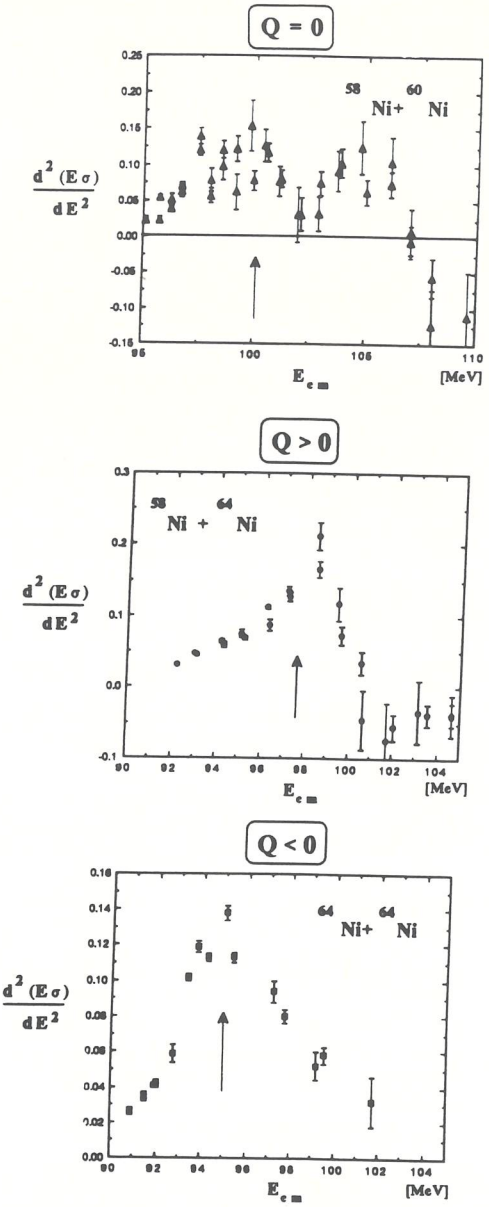

Figure 9: *Barrier distributions for the three indicated systems(normalized to πR^2).*

barrier. In particular we can identify the coupled transfer channels which act as doorway states for fusion, by means of the significant behaviour of $D(B)$ for different Q-values of these reactions, comparing the results with "exact" coupled channels calculations.

For the two more massive system we measured also the average angular momenta $< l > (E)$. As an further application of the barrier distributions method we derived $< l > (E)$ using D(B) as an effective potential [17] and compared this in a first attempt with our data. The comparison (fig. 10) works pretty well for $^{58}Ni+^{64}Ni$, whereas for $^{64}Ni+^{64}Ni$ especially in the low energy region a slight discrepancy occurs.

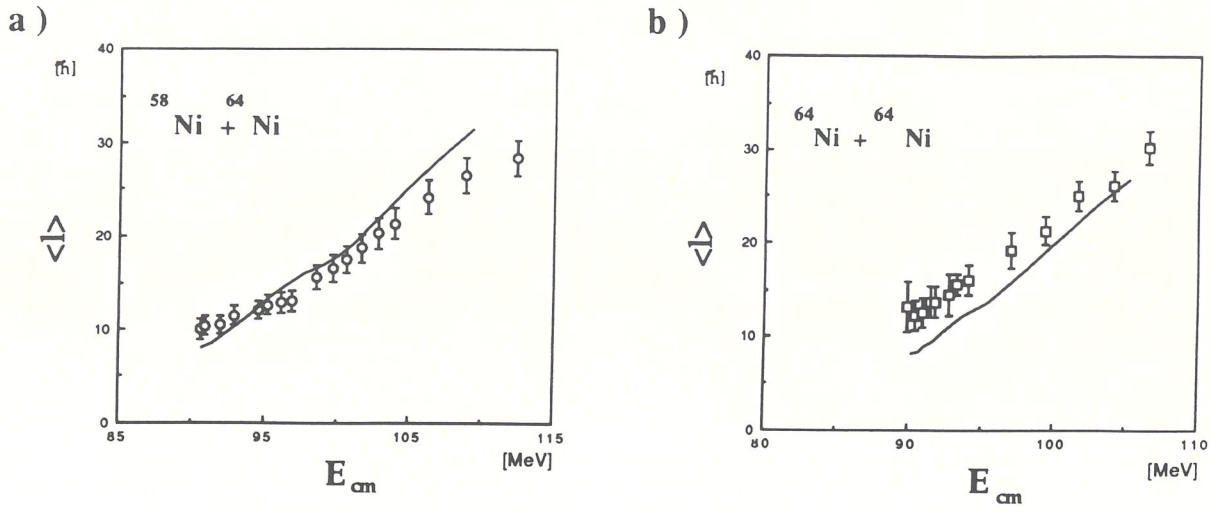

Figure 10: *Comparison between measured mean spins (data points) and the values derived from $D(B)$ (solid line) for a) $^{58}Ni+^{64}Ni$ and b) $^{64}Ni+^{64}Ni$.*

We like to thank Neil Rowley for many hours of fruitful discussions.

This work is a part of the Ph.D. thesis of D. Ackermann.

References

[1] R.G. Stokstad, Y. Eisen, S. Kaplanis, D. Pelte, U. Smilansky and I. Tserruya, Phys. Rev. C**21**, 2427 (1980).

[2] R.G. Stokstad, W. Reisdorf, K.D. Hildenbrand, J.V. Kratz and G. Wirth Z. Phys. A**295**, 269 (1980).

[3] W. Reisdorf, F.P. Heßberger, K.D. Hildenbrand, S. Hofmann, G. Münzenberg, K.-H. Schmidt, J.H.R. Schneider, W.F.W. Schneider, K. Sümmerer and G. Wirth, Nucl. Phys. A**438**, 212 (1985).

[4] J.S. Lilley, "Heavy-Ion Reactions near the Coloumb Barrier", *Proc. of the Study Weekend "Requiem for an Accelerator", 12./13. March 1993, SERC Daresbury Laboratory, Warrington (UK)*, to be published.

[5] A.M. Stefanini, G. Fortuna, R. Pengo, W. Meczynski, G. Montagnoli, L. Corradi and A. Tivelli, Nucl. Phys. A**456**, 509 (1986).

[6] A.M. Stefanini, L. Corradi, D. Ackermann, A. Facco, F. Gramegna, H. Moreno, L. Müller, D.R. Napoli, G.F. Prete, P. Spolaore, S. Beghini,

D. Fabris, G. Montagnoli, G. Nebbia, J.A. Ruiz, G.F. Segato, C. Signorini and G. Viesti, Nucl. Phys. **A548**, 453 (1992).

[7] D.E. DiGregorio and R.G. Stokstad, Phys. Rev. C**43**, 265 (1991).

[8] N. Rowley, G.R. Satchler and P.H. Stelson, Phys. Lett. **B245**, 25 (1991).

[9] N. Rowley, I.J. Thompson and G. Baggeley, *Proc. of the Workshop on the Physics and Techniques of Secondary Nuclear Beams, Dourdan, France, 23-25 March 1992*, to be published.

[10] R. Broglia, C.H. Dasso and S. Landowne, Phys. Rev. C**32**, 1426 (1985).

[11] S. Beghini, C. Signorini, S. Lunardi, M. Morando, G. Fortuna, A.M. Stefanini, W. Meczynsky and R. Pengo, Nucl. Instr. Meth. **A239**, 585 (1985).

[12] P. Spolaore, J.D. Larson, C. Signorini, S. Beghini, Zhu Xi-Kai and Si Hou-Zhi, Nucl. Instr. and Meth. **A238**, 381 (1985).

[13] A. Guerrieri, G. Maron, G. Montagnoli, D.R. Napoli and G.Prete, Nucl. Instr. and Meth. **A238**, 133 (1990).

[14] C.Y. Wong, Phys. Rev. Lett. **31**, 766 (1973).

[15] N. Rowley, L.J. Thompson and M.A. Nagarajan Phys. Lett. **B282**, 276 (1992).

[16] I.J. Thompson, Comp. Phys. Rep. **7**, 167 (1988).

[17] N. Rowley, private communication.